# Acoustic emission detection using intensity-modulated DFB fiber laser sensor

**Tan Yang (杨 郯)[1], Ying Song (宋 颖)[1], Wentao Zhang (张文涛)[2,*], and Fang Li (李 芳)[2]**

[1]*School of Traffic and Transportation, Shijiazhuang Tiedao University, Shijiazhuang 050043, China*
[2]*Optoelectronic System Lab, Institute of Semiconductors, Chinese Academy of Sciences, Beijing 100083, China*
**Corresponding author: zhangwt@semi.ac.cn*

Received August 27, 2016; accepted October 14, 2016; posted online November 14, 2016

The bonded distributed feedback (DFB) fiber laser (FL) acoustic emission sensor and the intensity response of the DFB-FL to external acoustic emissions are investigated. The dynamic sensitivity of the DFB-FL is calibrated by a referenced piezoelectric receiver. In the DFB-FL we used here, the minimum detectable signal is $2 \times 10^{-6}$ m/s at 5 kHz. Using wavelet packet technology, the collected signals are analyzed, which confirms that an intensity-modulated DFB-FL sensor can be used to detect acoustic emission signals.

*OCIS codes: 060.2370, 140.3490, 140.3510.*
*doi: 10.3788/COL201614.120602.*

The acoustic emission (AE) technique as a kind of new nondestructive testing technology has a broad potential application in the field of nondestructive testing. Traditional AE sensors are usually made of piezoelectric (PZT) ceramic materials, which are not only susceptible to electromagnetic interference, but also unsuitable for being embedded into structures. Fiber optic sensors have considerable advantages over traditional PZT sensors, such as a small diameter, light weight, flexibility, immunity to electromagnetic interference, durability, ease of installation and multiplexing, and a simultaneous measurement of temperature and strain[1–5]. These characteristics are very suitable for real-time health monitoring of structures in their service life cycle[3,6]. Recently, distributed feedback (DFB) fiber laser (FL) -based sensors, including strain sensing[6,7], and acoustic sensors[8–10] have attracted a lot of interest due to their higher resolution. Compared with the fiber Bragg grating (FBG), DFB-FL sensors have an ultra-narrow line-width and higher output power, which result in an ultrahigh strain resolution[11,12]. Many papers use the interference method of demodulation, however, the method of demodulation system is complex, and the cost is high. Using the intensity characteristics of the DFB-FL to detect a signal, the demodulation system is simple, and the detection of the signal frequency band is wide[13].

In this Letter, we present the bonded intensity response of the DFB-FL to the external AE signal, and the acoustic measurement based on the AE is done on an aluminum plate to prove the feasibility of the sensing scheme. We reveal the sensitivity response curve of the intensity-type DFB-FL sensor to external AE signals and explain the minimum of the stress wave that can be detected by the method.

First, we explain the focus of this Letter, which is to use the intensity characteristics of the DFB-FL as the receiver of the AE signal. When there is external AE signal applied on the phase-shift grating, the fiber is physically stressed due to the elasticity of the fiber, and the refractive index of the fiber is modified because of the photo-elasticity[14]. The relationship between the length of the fiber grating ($l$), the refractive index ($n$), and the elastic wave can be expressed as

$$\begin{aligned} \Delta l(t) &= l_0 - \frac{(1-2\mu)P_{(t)}l}{E}, \\ \Delta n_{(t)} &= n_0 + \frac{n^3 P_{(t)}(1-2\mu)(2P_{12}+P_{11})}{2E}, \end{aligned} \tag{1}$$

where $P_{(t)}$ is the amplitude of the elastic waves, $E$ is the Young's modulus of the fiber, $P_{11}$ and $P_{12}$ are elasto-optical coefficients, and $\mu$ is Poisson's ratio of the fiber.

Therefore, the grating coupling coefficient and the refractive index of the FL influences its output power. As a result, the effect of the external AE signal modulation, which may contribute significantly to the DFB-FL's intensity, should be analyzed and discussed.

As shown in Fig. 1, a 980 nm pump laser is used before the wavelength division multiplexer. The output laser of the DFB-FL goes through the isolator, wavelength division de-multiplexer, and into the detector. The analog/digital (A/D) card is used to sample the output voltage signal of the detector and transmit the signal to the personal computer (PC). The collective digitized signal is then processed using the Fourier transform to evaluate

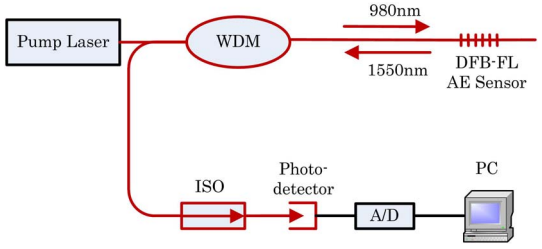


Fig. 1. Intensity FL AE sensing scheme. ISO, isolator.

 

the AE signal components. The sensitivity of the DFB-FL AE sensor to the external AE signal is tested. Experimental results of a high sensitivity and a high accuracy are obtained.

The intensity characteristics of the DFB-FL include the relative intensity noise (RIN) of the output laser and the intensity response characteristics of the external pressure excitation. The characteristic of RIN plays an important role in the sensitivity of the sensor. The length and refractive index of the fiber grating can be changed when the external AE is excited in the DFB-FL, which can cause the fluctuation of the output power of the DFB-FL. Finally, the RIN spectrum is obtained by the software program in the computer. The RIN is given by

$$\mathrm{RIN}^2(f) = \Delta\mathrm{RI}^2(f), \tag{2}$$

where $\Delta\mathrm{RI}\,(f)$ is due to the relative fluctuation of the output laser power, and the power spectrum density is obtained after the Fourier transform.

The DFB-FL has excellent sensing properties, such as anti-electromagnetic infection, high temperature resistance, ease of wavelength division multiplexing, and so on. But, its own structure is thin and easy to break. This Letter designs a kind of bonded sensor to protect the FL, as shown in Fig. 2. We select the small elastic modulus of the substrate material to package the bonded-type sensor, which can not only be effective in the compensability of the elastic wave, but can also be very good at protecting the DFB-FL.

In order to investigate the intensity response of the DFB-FL to AE signal, first, the relative noise of the system is evaluated, and then by comparing that with the PZT sensor, the sensitivity curve of the test band is obtained. Finally, the burst signal by the DFB-FL AE sensor is aquired.

The experiment of AE sensitivity calibration is carried out on a square aluminum plate, as shown in Fig. 3. The

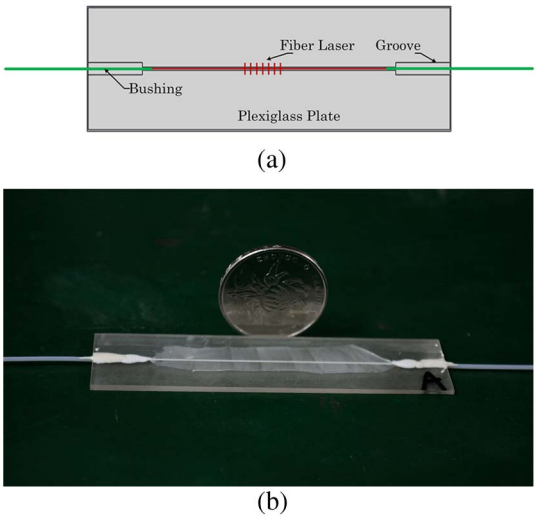


Fig. 2. (a) Structure of the bonded DFB-FL sensor. (b) Bonded DFB-FL AE sensor.

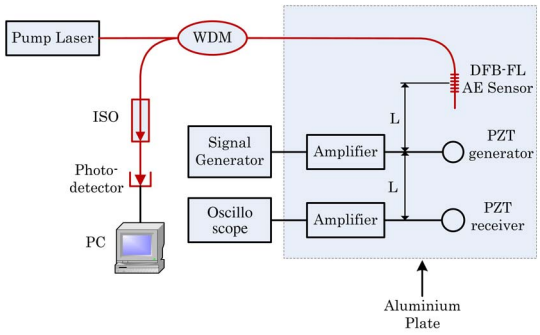


Fig. 3. Detection of AE waves in an aluminum plate.

DFB-FL AE sensor is fixed on the aluminum plate. Two PZT AE transducers, one working as the AE generator and another working as AE receiver, are glued to the aluminum plate. The distances between the AE generator and the two receivers (the DFB-FL receiver and the PZT receiver) are the same.

A 5.1 kHz sinusoidal signal is generated by a signal generator and collected by the DFB-FL AE sensor and the PZT receiver. The AE sensitivity of the PZT receiver is expressed as Eq. (3), which is 69.75 dB re V/m/s at 5.1 kHz:

$$M = 20 \times \lg\left(\frac{e}{P}\right), \tag{3}$$

where $e$ is the voltage detected by the PZT receiver. Then, the AE $P$ is calculated as 0.00026 m/s, according to Eq. (3).

Figure 4 shows the experimental result of the intensity response of the bonded DFB-FL sensor to the AE excitation, which is 0.00026 m/s as mentioned above. We can

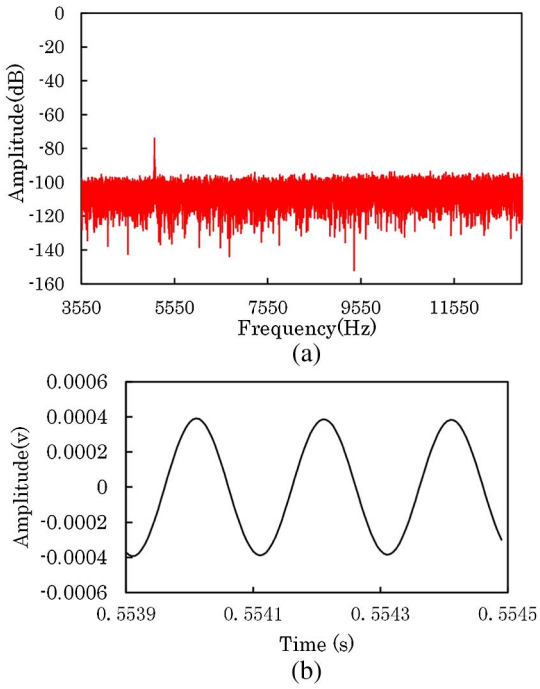


Fig. 4. (a) Frequency domain characteristics of the 5 kHz Signal. (b) Time domain characteristics of the 5 kHz AE signal.

directly observe the 5.1 kHz signal with 25 dB in the DFB-FL RIN spectrum. The collected signal is well presented in the time domain characteristics of the applied signal. The experimental results show that the bonded sensor not only has good sensing properties, but can also protect the optical fiber.

The sensitivity of the DFB-FL AE sensor is calibrated by comparing the received signals of the PZT AE sensor and the DFB-FL AE sensor when the AE generator is driven by a specific voltage. The sensitivity of the DFB-FL AE sensor is expressed as

$$M_{\mathrm{DFB}} = 10 \times \lg\left(\frac{P_s}{P}\right), \tag{4}$$

where $P_s$ is the DFB-FL output power, and $P$ is the AE amplitude.

By testing the AE waves at different frequency points, the frequency response of the DFB-FL AE sensor is obtained, which is shown in Fig. 5.

Then, the AE sensitivity at 5.1 kHz can be calculated as 17.96 dB re mW/m/s. The decibels (dB) in Fig. 5 represent a relative value, and 0 dB is 1 mW by calculating Eq. (4). As shown in Fig. 5, we show the sensitivity response curve of the intensity-type DFB-FL sensor to the external AE signal at frequencies between 1 and 9 kHz. Because we select the small elastic modulus of the substrate material to package the bonded type sensor, it is not only effective in the propagation of the elastic wave, but also can't be easily to be influenced by environment. So, the bonded sensor's sensitivity curve is closer to the PZT sensitivity curve than the two fixed ends, as shown in Fig. 5. The small changes of the power system resolution play an important role in determining the minimum detectable signal. The minimum resolution of the demodulation system is $1 \times 10^{-4}$ mW. The minimum detectable AE signal is $2 \times 10^{-6}$ m/s at 5 kHz.

In addition, the sensor will be used to detect the AE signals of rock mass in a future work. The rock AE signal is mainly at a low frequency. Finally, we use the shocked steel ball method to simulate the burst AE signal. In the experiment, the burst type AE signal generated by the shocked steel ball is transmitted to the DFB-FL AE sensor and the PZT receiver through the surface of the aluminum plate. Figures 6(a) and 6(b) show that the DFB-FL AE sensor and the PZT receiver respond to the burst signal.

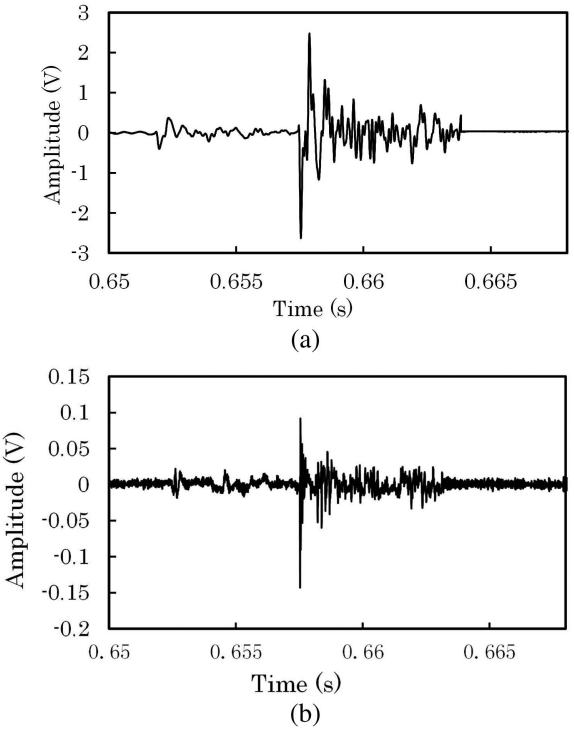


Fig. 6. (a) Signal of a shocked steel ball by the PZT sensor, (b) Signal of a shocked steel ball by the bonded DFB-FL sensor.

In order to show the frequency of the signal acquisition, we have carried out the fast Fourier transform, as shown in Fig. 7. The results show that the signals collected by the two sensors are in the same frequency. The noise level of the DFB-FL AE sensor is lower than the PZT receiver. The DFB-FL is more conducive to detecting the AE signal.

In conclusion, we present our recent work on the DFB-FL-based AE sensor. With the intensity modulated type FL sensor, we obtain a high frequency response AE detection system with the benefits of simplicity in

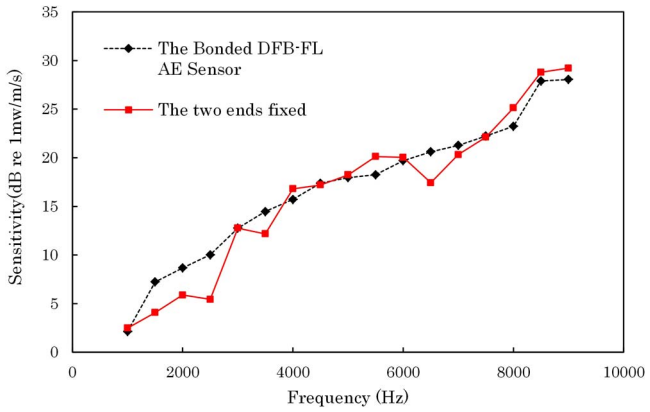


Fig. 5. Sensitivity response curve of the intensity-type DFB-FL sensor to external AE.

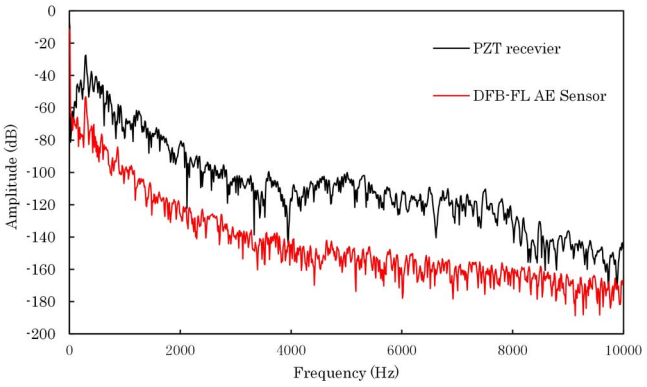


Fig. 7. Fast Fourier transform of the signal.

demodulation and multiplexing. The minimum detectable signal is tested to be better than $2 \times 10^{-6}$ m/s at 5 kHz. The results show that the intensity-modulated-type FL is suitable in low-cost industrial applications.

This work was supported by the National 863 Program of China (No. 2014AA093406), the Youth Innovation Promotion Association of CAS (No. 2016106), the Project of Observation Instrument Development for Integrated Geophysical Field of China Mainland (No. Y201606), and the Key Project of Hebei Educational Committee (No. BJ2016048).

## References

1. W. Z. Huang, H. X. Ma, W. T. Zhang, F. Li, and Y. L. Du, in *Advanced Sensor Systems and Applications V* (2012).
2. P. Finkel, R. Miller, R. D. Finlayson, and J. Borinski, AIP Conf. Proc. **557**, 1844 (2001).
3. X. Zhang, F. Zhang, S. Li, M. Wang, L. Wang, Z. Song, Z. Sun, H. Qi, C. Wang, and G. Peng, Chin. Opt. Lett. **12**, S10608 (2014).
4. Z. Yang, H. Sun, T. Gang, N. Liu, J. Li, F. Meng, X. Qiao, and M. Hu, Chin. Opt. Lett. **14**, 050604 (2016).
5. W. He, L. Cheng, Q. Yuan, Y. Liang, L. Jin, and B.-O. Guan, Chin. Opt. Lett. **13**, 050602 (2015).
6. H. Tsuda, E. Sato, T. Nakajima, H. Nakamura, T. Arakawa, H. Shiono, M. Minato, H. Kurabayashi, and A. Sato, Opt. Lett. **34**, 2942 (2009).
7. G. M. H. F. Geoffrey, A. Cranch, and C. K. Kirkendall, IEEE Sens. J. **8**, 1161 (2008).
8. W. Z. Huang, W. T. Zhang, and F. Li, Sensors **13**, 14041 (2013).
9. P. P. Wang, J. Chang, C. G. Zhu, W. J. Wang, Y. J. Zhao, X. L. Zhang, G. D. Peng, G. P. Lv, X. Z. Liu, and H. Wang, Laser Phys. Lett. **9**, 596 (2012).
10. Q. Wu and Y. Okabe, Opt. Express **20**, 28353 (2012).
11. D. J. Hill, B. Hodder, J. De Freitas, S. D. Thomas, and L. Hickey, in *17th International Conference on Optical Fibre Sensors, Pts 1 and 2* (2005), p. 904.
12. W. Z. Huang, W. T. Zhang, H. X. Ma, F. Li, and Y. L. Du, Appl. Mech. Mater. **330**, 412 (2013).
13. J. Z. Zhang, X. L. Li, Q. A. Chai, Q. Q. Hao, Q. Li, W. M. Sun, L. B. Yuan, P. Lu, and G. D. Peng, in *2010 IEEE Sensors* (2010), p. 315.
14. N. Takahashi, K. Yoshimura, S. Takahashi, and K. Imamura, Ultrasonics **38**, 581 (2000).